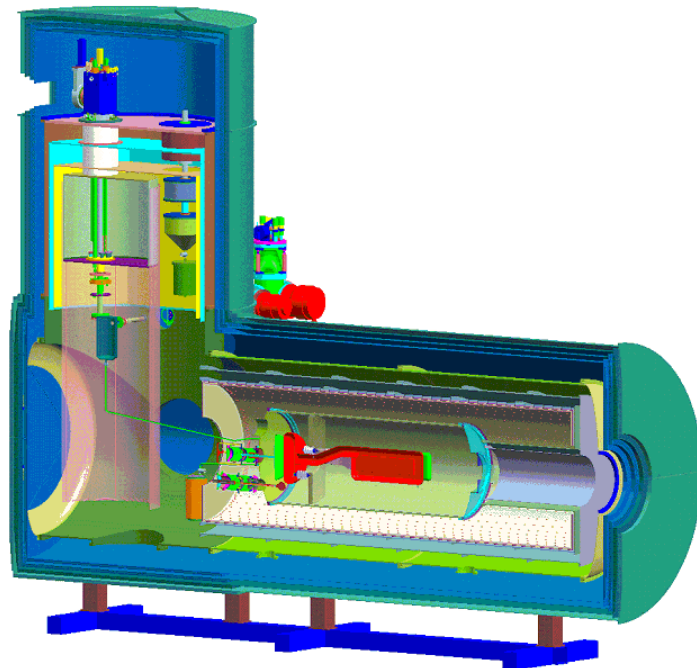


# **A New Search for the Neutron Electric Dipole Moment**

## **Report: Recent Progress and Design Changes**

Prepared  
by  
**The Neutron EDM Collaboration**

February 1, 2005



This report has been submitted to:  
The LANL Internal EDM Committee:  
Review of Cost and Schedule

LANL Committee Meeting: February 11, 2005

## **Document Overview**

In March 2002, the Neutron EDM Collaboration prepared a research and funding pre-proposal for submission to the Office of Science in the Department of Energy. This document addressed the scientific motivation, technical approach, and initial engineering solutions for a new measurement of the neutron electric dipole moment. In the intervening three years, many of the concepts described in the proposal have been explored, validated, and fleshed out in more detail. In some cases, a more detailed analysis has suggested a better engineering design. The purpose of this document is to complement the document written in 2002 and to provide details on new insights into the optimum design of the experiment.

This document is not intended to stand alone but should be read as a companion report to the research and funding pre-proposal. It is intended to clarify and document our updated reference design for the experiment as of February 2005. In some areas, design work is still in progress. These tasks are not addressed here but are identified at the end of this report.

A modified cost analysis for the neutron EDM project will be provided in a separate document.

## Table of Contents

Section	Page
I. Introduction	4
II. New Reference Design	
A. General Layout and Design Changes	6
B. Dressed Spin Measurement Technique	9
III. Measurement Strategy at SNS	
A. General Considerations	11
B. Operation at the SNS 8.9 Angstrom beam line	11
IV. R&D Results – Short Summaries	
A. HV Test Apparatus and Measurements	13
B. Kerr Effect in Superfluid $^4\text{He}$	17
C. Magnetic Fields and Magnetic Shielding	19
D. Test and Performance of the $^3\text{He}$ Atomic Beam Polarizer	21
E. $^3\text{He}$ Cell Studies	24
F. Reservoir for Purification of Superfluid $^4\text{He}$	26
G. Background Issues	28
H. $^3\text{He}$ Polarization Losses in the $^3\text{He}/^4\text{He}$ Sample Preparation Volume	31
V. Additional Investigations in Progress	34
VI. Conclusions	34

## I. Introduction

A research and funding pre-proposal for a new experiment to search for the neutron electric dipole moment (EDM) was submitted to the DOE on March 22, 2002. That document presents the basic scientific and technical challenges associated with this new experiment. Here we present a concise update of the project including recent scientific and technical developments that have occurred since the pre-proposal was submitted.

A thorough review of fundamental neutron science opportunities was carried out by a sub-committee of the Nuclear Science Advisory Committee (NSAC) in 2003. The subcommittee received the DOE EDM pre-proposal and heard presentations from members of the EDM collaboration. The report from this sub-committee strongly endorsed this new search for the neutron EDM. Quoting from the subcommittee report:

*The subcommittee found the science to be very compelling: The EDM experiment has the highest discovery potential of all proposed experiments. The subcommittee strongly supports it. We encourage the collaboration to address the technical issues surrounding this experiment and recommend that R&D funding be provided to accomplish this.*

Since the submission of our pre-proposal, the scientific impact of improving the limits on the neutron EDM remains high. With nearly six orders-of-magnitude between the present best limit and the predictions from the Standard Model, there is ample opportunity for new physics to be observed. Several European efforts are under discussion to improve on the existing limits. These include a new liquid He based experiment, similar to our technique that is under development at ILL, and a solid deuterium-based experiment at PSI that is under discussion. The relative competitiveness of the ILL and PSI projects with the technique discussed here is not addressed in this report.

During the presentations to the NSAC subcommittee, the collaboration reviewed areas of technical risk and identified seven areas for research and development (R&D) where poor results could substantively reduce the sensitivity of the apparatus. These were:

1. Initial polarization of  $^3\text{He}$
2. Strength of static electric field
3. Impact of a beta decay background on the neutron- $^3\text{He}$  capture signal
4. Spin relaxation time of  $^3\text{He}$
5. Shielding of magnetic fields
6. Neutron wall losses
7. Noise level in SQUID detectors

Important advances in design and technique, developed by our collaboration, have improved our understanding of the feasibility of the experiment. Of the R&D areas, the collaboration feels that achieving the  $^3\text{He}$  initial polarization (1) and the strength of the static electric field (2) have been demonstrated to be achievable. The identification of

neutron absorption products (3) has been demonstrated if we can achieve good photo-electron statistics. Very encouraging preliminary results have been achieved for the  $^3\text{He}$  spin-relaxation time (4) and for trapped gradient fields (5). Investigations of the impact of neutron wall losses (6) and the SQUID noise level (7) are in progress but are expected to be achievable. Note that the degradation in sensitivity for the last two was estimated at the time of the NSAC Review to be factors of 1.8 and 1.6, respectively. Hence, the overall technical risk has been greatly reduced by the recent R&D investigations. These studies continue to improve our understanding of the limitations of the measurement as well as to inspire new concepts for inclusion into the apparatus.

In parallel to the R&D activities, the collaboration's understanding of the experiment has been greatly aided by pre-conceptual engineering to identify any conflicts introduced by placing all the components into a single piece of equipment. Progress in the R&D program is briefly reported in this document. The collaboration is convinced that there are now no technical "show-stoppers" in the concept of the experiment.

## II. New Reference Design

### A. General Layout and Design Changes

The EDM experiment reference design has evolved considerably as we have proceeded to demonstrate that the entire suite of physics ideas can be built into a single apparatus. In this section, we briefly point out where there is a significant change of design and the motivation behind design changes since development of the March 2002 pre-proposal.

#### 1. Neutron Beam Line Configuration

The collaboration is now focused on designing for and operating the experiment solely at the SNS. This has resulted in some simplification and improvement in the beam line configuration. The neutron beam emerging from the biological shield (see Fig. II.A.1.) passes through a Bismuth Filter, a ballistic neutron guide section, and a neutron beam splitter guide section (spin filter) which is matched to the EDM apparatus.

The existence of the upstream Bragg monochromators at the SNS eliminates the need for both the frame overlap and  $T_0$  choppers that were planned for LANSCE. The Bi filter (or a second chopper) is still in use to eliminate the shorter wavelength ( $n=2, \dots$ ) neutrons that pass the monochromators. The optimum position of the Bi filter or second chopper is under study.

At SNS, the full beam splitter, which is about 14 m in length, is part of the design. The increase from 4 to 14 m drives a cost increase, but the performance is greatly improved. As shown in Fig. II.A.1, the splitter extends well into the main guide hall.

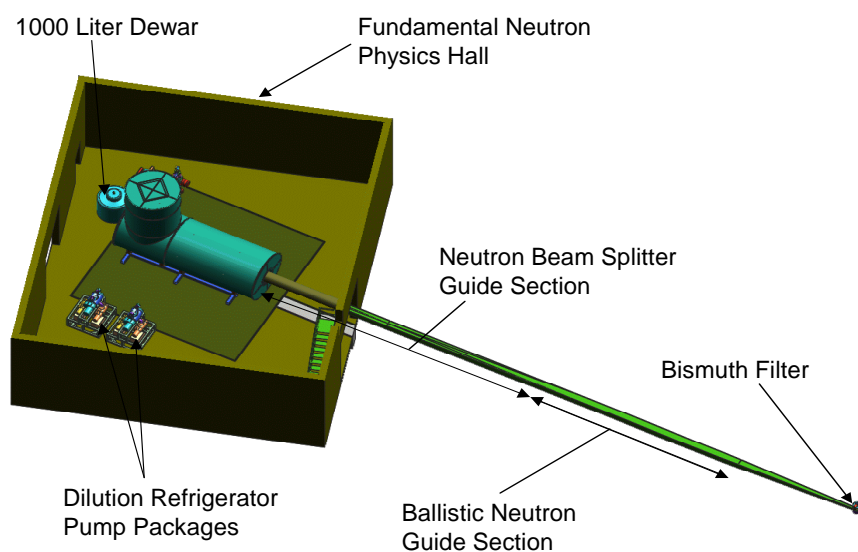


Figure 1

Figure II.A.1. Neutron Beam Layout at SNS

## 2. Lower Cryostat Design

Important changes in the EDM measurement apparatus have also occurred. The lower cryostat, where the trapped neutron measurement cells are located, is shown in Fig. II.A.2. A detailed discussion of a series of tests and design changes are presented in Section IV (see Fig. IV.C.1); we present here a few of the main points. The high voltage (HV) system has been made coaxial with the center of the cryostat. This alignment minimizes the length of the cable between the multiplying capacitor and the cell electrodes, thus reducing the capacitance of this connecting line so that the high voltage on the electrodes is as high as possible (see Section IV.A).

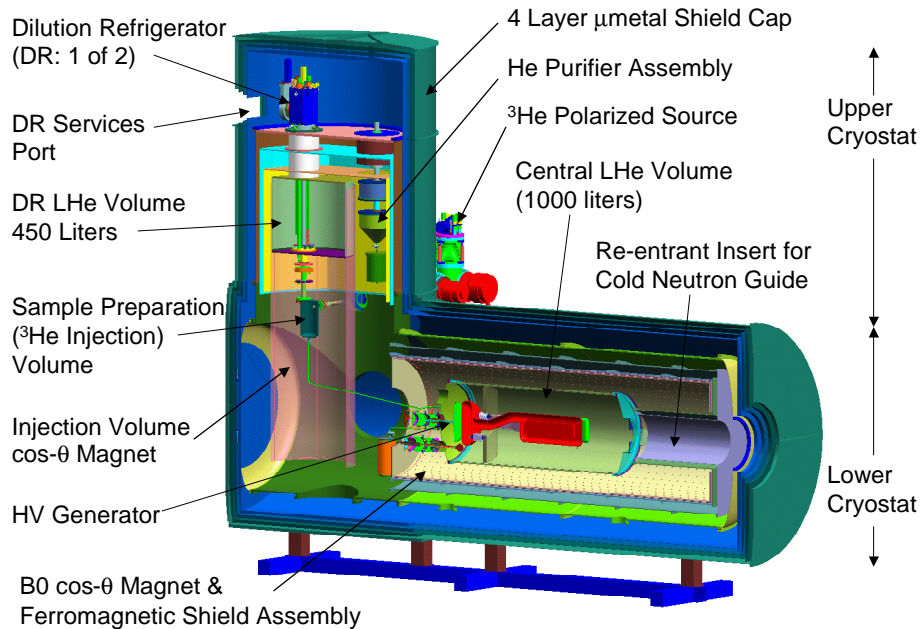


Figure II.A.2. Neutron EDM measurement apparatus

Detailed studies in the design of the  $\cos\theta$  coils for the static B field have revealed that they can be built with open ends (see Section IV.C). As a result, we have been able to redesign the lower cryostat to have a reentrant insert to allow the neutron guides to come as close to the measurement cells as allowed by the high voltage considerations. Thus the nagging problem of a need for cryogenic super-mirror guides has been avoided.

The magnetic field coils and shielding has been dramatically redesigned. It now consists of (Fig. IV.C.1): a nested set of a (double) RF coil system, a static field coil, a ferromagnetic shield, and a superconducting shield. The motivation for these changes is addressed in detail in Section IV.C. The addition of the extra elements has substantially increased the size of the lower cryostat to a length of 8.4 m and a diameter of 3.2 m.

### 3. Upper Cryostat

The upper cryostat contains the dilution refrigerators (DRs) and  $^3\text{He}$  manipulation volumes. In anticipation of a very tight heat budget, the collaboration has decided that providing for a second DR is appropriate. The upper cryostat has been moved downstream of the lower cryostat to minimize the field distortions due to service penetrations. The multiple cold heads in our earlier design have been replaced with a liquefier in order to improve the refrigeration and minimize vibrations. The service connections between the liquefier and the DRs have been bent at  $180^\circ$  inside the magnetic shielding to isolate magnetically the apparatus from the outside environment. The upper cryostat reaches to a height of 7.2 m and has a 3.0-m diameter.

Inside the upper cryostat, Figs. II.A.2 and IV.F.1, there are a number of new or more highly developed volumes for  $^3\text{He}/^4\text{He}$  management included in the design. We discuss here the  $^4\text{He}$  purification volume and the  $^3\text{He}/^4\text{He}$  sample preparation volume.

The removal of depolarized  $^3\text{He}$  is now done by pumping on the volume above the  $^3\text{He}/^4\text{He}$  fluid (see Section IV. F). A conical shape maximizes the ratio of the top-surface area to the volume. The pumping is done with a  $\sim 4$  K activated-charcoal trap. The strategy of pumping on the  $^3\text{He}$  arose from our measurement of the diffusion coefficient of  $^3\text{He}$  in superfluid  $^4\text{He}$ , [1]. Effective  $^3\text{He}$  removal will be realized if the velocity in this temperature region is sufficient to overcome the binding energy of the  $^3\text{He}$  in the liquid. The second DR will give us enough cooling power to return to the heat flush technique if the evaporative method is inadequate.

The volume for  $^3\text{He}$  injection and sample preparation has been carefully studied. We plan to have the walls of the injection region coated with superfluid  $^4\text{He}$  that rises out of the liquid via the HEVAC effect. The technique needs to be tested, but our expectation is that the circulating superfluid will carry the polarized  $^3\text{He}$  into the liquid.

The circulation of the superfluid needs to be controlled in both the sample preparation and evaporation volumes. The control is provided by film burners that supply heat in a restricted region of the vessels. However the heat generated is a significant load on the DRs. A new  $\cos\theta$  magnet surrounding the sample preparation volume has been added to preserve the polarization of the  $^3\text{He}$ . This magnet extends through most of the upper cryostat and must have relatively high uniformity.

- [1] S.K. Lamoreaux et al, "Measurement of the  $^3\text{He}$  mass diffusion coefficient in superfluid  $^4\text{He}$  over the 0.45-0.95 K temperature range," *Europhysics Letters* 58, 718 (2002).

## II.B. Dressed Spin Measurement Technique

As described in the pre-proposal, the experimental signal from the capture of polarized neutrons on polarized  $^3\text{He}$  atoms is modulated by the difference in magnetic moments of the two species. In order to determine the actual neutron precession frequency, the magnetic field must of course be known; in the pre-proposal we described an independent measurement of the  $^3\text{He}$  precession frequency using NMR with SQUID pickup-coils for this purpose.

In addition to this use of the  $^3\text{He}$  atoms as a co-magnetometer, we propose to implement a dressed<sup>1</sup> spin measurement system in the experiment. For this purpose, an alternating current, AC, magnetic field is introduced in addition to the constant field,  $B_0$ , the effect of which is to change the effective magnetic moments of neutrons and  $^3\text{He}$  atoms [1]:

$$\gamma_{eff} = \gamma_0 J_0 \left( \frac{\gamma_0 B_{AC}}{\omega_{AC}} \right)$$

where  $\gamma$  is the gyromagnetic ratio and  $J_0$  is the ordinary Bessel function of zero order. The effective neutron magnetic moments in AC fields have been measured at ILL [2]. Of particular interest is the solution for which the effective neutron and  $^3\text{He}$  magnetic moments are equal

$$\gamma_{0,n} J_0 \left( \frac{\gamma_{0,n} B_{AC}}{\omega_{AC}} \right) = \gamma_{0,3} J_0 \left( \frac{\gamma_{0,3} B_{AC}}{\omega_{AC}} \right) \Rightarrow \frac{\gamma_{0,n} B_{AC}}{\omega_{AC}} = 1.19$$

which defines a critical AC frequency. Small random or systematic changes in  $B_0$  dictate that the AC frequency be 100 or more times the nominal precession frequency; we choose  $\omega_{AC} = 2\pi \cdot 1 \text{ kHz}$ . At the critical AC frequency, the n- $^3\text{He}$  capture rate decreases to zero. In practice one would sweep the AC frequency about the critical value to determine the neutron precession rate (separately for each state of  $\vec{B} \cdot \vec{E}$ ).

During the experiment, both methods (dressed spin and SQUID measurements) for determining the neutron precession frequency in the holding field would be used to determine the electric dipole moment signal.

In order to implement this dressed spin technique, we plan to add a pair of additional cos- $\theta$  coils to produce the required AC field perpendicular to the holding field:

$$\vec{B}_0 = B_0 \hat{x}, \quad \vec{B}_{AC} = B_{AC} \hat{y}$$

with the neutron beam axis along  $\hat{z}$  (these coils can also be used to generate the  $\pi/2$  flip pulse). We have designed a system of two ‘dressing’ coils (with opposite current senses) with radii differing by  $\sim 15 \text{ cm}$  in order to reduce the eddy current heating of the AC

---

<sup>1</sup> “Dressed” systems are ones in which photons are coupled approximately (i.e. not in the full field theoretic sense) to the matter system of interest – dressed spins were introduced Cohen-Tannoudji and Haroche in 1969.

fields in the shields to manageable levels [3]. The uniform inner AC field can be set to the required  $|B_{AC}| = 0.4 \text{ G}$  and the outer field approximately canceled by the second AC coil, with the resulting dissipation of  $< 1 \text{ W}$  in the ferromagnetic shield ( $T = 4 \text{ K}$ ). For the same reason, the AC fields also set limits on the (minimum) resistance of the conductive coating for the electric field electrodes ( $T = 0.3 \text{ K}$ ) at about  $1 \text{ } \Omega$  (or a resistivity of  $\sim 100 \text{ m}\Omega\cdot\text{cm}$ ). The conducting coating on the electrodes cannot in any case have very low resistance because of the thermal magnetic field noise requirements of the SQUIDs.

We believe this combination of coils and shields will preserve the option to test both the SQUID method and the dressed field method for measuring the neutron spin precession in a controlled magnetic field environment.

Several tasks remain in the development of the dressed spin technique including

- i. Continued development of the coil design and detailed calculations of the heating effects,
- ii. Measurement of the dressing effect on  $^3\text{He}$  using the atomic beam source at LANL,
- iii. Simulation of a dressing measurement in the EDM apparatus.

[1] R. Golub and S. Lamoreaux, Phys. Rep. 237 1 (1994).

[2] E. Muskat, D. Dubbers, and O. Sharpf, Phys. Rev. Lett. 58 2047 (1987).

[3] C.P. Bidinosti, I.S. Kravchuk, J. Cha, N.A. David, and M.E. Hayden, Wire-Wound B1 Coils for Low Frequency MRI, pg 1551, Proceedings of the 12th Meeting of the International Society for Magnetic Resonance in Medicine (Kyoto, Japan, 2004);

"Active Shielding of Cylindrical Saddle-shaped Coils," C.P. Bidinosti, I.S. Kravchuk, and M.E. Hayden, J. Magn. Reson. (To be submitted).

### **III. Measurement Strategy at SNS**

#### **III.A. General Considerations**

The pre-proposal assumed a two-phase approach to the EDM experiment. In this scheme, the experiment would operate first at the Los Alamos Neutron Scattering Center, where beam is regularly available. Afterwards, the experiment would be moved to the Spallation Neutron Source (SNS) at Oak Ridge National Laboratory, an accelerator under construction that promises greatly improved intensity.

The current funding plan for the EDM experiment calls for an EDM construction start in FY'07 and for commissioning in FY'11. This schedule is now consistent with mounting the experiment only at the SNS. Some noticeable savings come from not having to move and rebuild the apparatus. Additionally, the SNS guide hall has room for the complete beam splitter/polarizer, which allows for improved transmission and polarization.

The SNS will be the world's most intense pulsed neutron source, providing a neutron flux approaching that of a large research reactor. It is expected that the facility will produce its first neutrons in 2006. Beam Line 13 will be dedicated to fundamental neutron physics experiments.

#### **III.B. Operation at the SNS 8.9-Angstrom Beam Line**

The SNS Fundamental Neutron Physics Beam Line (FNPB) will have a separate beam line dedicated to experiments that will use the super-thermal process in superfluid liquid helium to produce UCN. Neutrons produced in the spallation target will travel through a straight section and a series of benders. After the first chopper, the 8.9-Angstrom neutrons will be selected by a double-crystal monochromator and will be sent to an external building located about 30 m downstream (see Figs. III.A.1 and II.A.1). The use of benders, which eliminates the line-of-sight views of the source, and the use of the monochromators, which eliminates the neutrons with the "wrong" wavelength, will minimize the background neutrons and other background radiation. In addition, since the source is pulsed, backgrounds can be studied with and without beam.

A straight section of guide will follow the double-crystal monochromator. As the beam exits the biological shield, it will pass through a second chopper or a bismuth filter to remove gamma rays and higher energy neutrons ( $n=2,3,\dots$ ) that pass the monochromators. The optimum position of the second chopper or Bi filter is under study.

Following the filter, the guide will have an expansion section for transition into a ballistic guide, which can transport neutrons for a large distance more effectively. The ballistic ( $m=1$ ) guide matches nicely to a beam splitter/polarizer. Preliminary designs of the splitter/polarizer indicate it will be about 14 m in length and transmit roughly 50% of the neutrons with good polarization ( $\sim 96\%$ ). Note that since the splitter/polarizer will project substantially into the main guide hall, there is a possibility that some beam-line project funds could assist with its cost.

The EDM experiment will be housed in the external building, Fig. III.A.1, provided by the FNPB, which will be equipped with: a vibrationally isolated floor slab for support of the experiment, cryogenic service, road access for experimental equipment, sufficient power

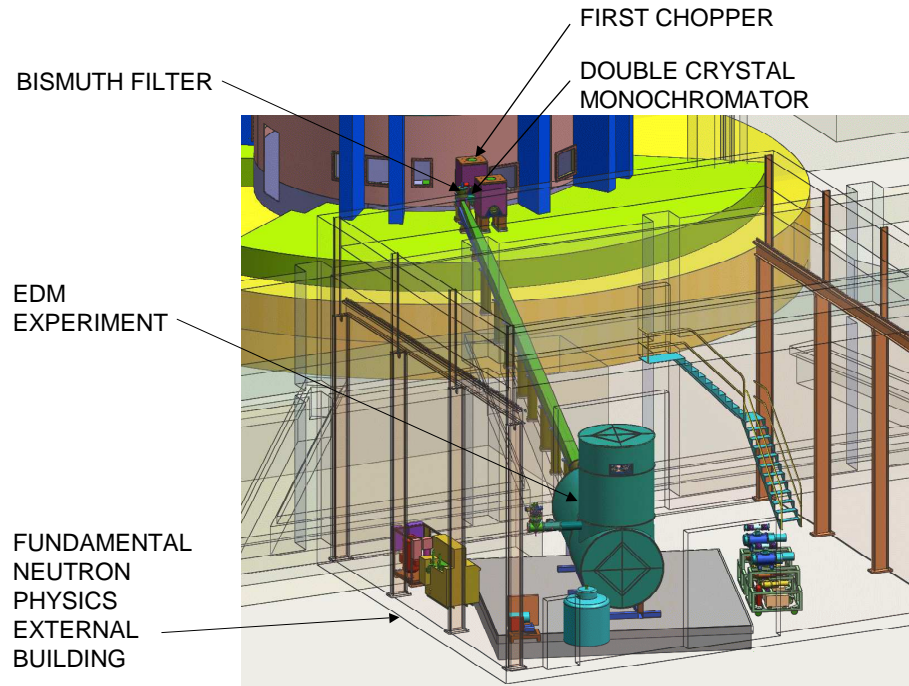


Figure III.A.1. Fundamental Neutron Physics Facility at SNS. Beam line 13. See Fig. II.A.1. for the layout of specific components of the neutron beam.

and a crane with the required hook height. The location, external to the main target building, will also significantly reduce backgrounds.

All of these factors at the SNS FNPB: unprecedented flux at a pulsed source, reduced beam related backgrounds, vibrational isolation, additional control over systematic errors, and a facility with all required services, will present the EDM project with an opportunity to achieve its fullest sensitivity to the neutron EDM.

## **IV. R&D Results – Short Summaries**

### **IV.A. HV Test Apparatus and Measurements**

Members of the EDM collaboration at Los Alamos completed in December 2003, the construction of an apparatus to measure the dielectric properties of large volumes of liquid helium and to prototype the high-voltage amplification system for the EDM experiment. The apparatus, Fig. IV.A.1, consists of a variable parallel-plate capacitor with  $1600\text{ cm}^2$  electrodes and a gap adjustable from 0 to 8 cm. It is contained in a 190-liter liquid helium vessel enclosed in a large-volume insulating vacuum chamber. Electrode separation is controlled by rods attached to bellows on the ends the vessel and vacuum chamber. This design is based on a strategy in which high voltages are generated by charging electrodes to a low voltage, isolating them, and then increasing the electrode spacing. This scheme is necessary since the cryogenic environment precludes the practical application of the necessary voltage directly to the electrodes using external power supplies and cable feedthroughs.

Several results were obtained on normal-state liquid helium (near 4 K) in February 2004. The amplification system was tested successfully. The electrodes were consistently charged to over 500 kV at their maximum separation of 8 cm, Fig. IV.A.2. This electric field (62 kV/cm) was nearly 30% higher than anticipated based on previous experiments with small volumes of liquid helium, and 30% higher than the target values for the EDM experiment. These potentials differences were maintained for long periods, decaying by less than 5% over 12 hours. This performance was well within the requirements of the experiment, and was only 3% of the maximum degradation tolerable in the EDM experiment. The high potentials were also obtained with a sealed neutron source in close proximity to the apparatus, indicating that the proposed HV technology for the EDM experiment will be sufficiently robust in an accelerator environment with a substantial background flux of stray neutrons.

In mid-2004, the apparatus was modified to include a custom liquid helium transfer line and a high-speed pump above the main volume, to attempt electrical tests on liquid helium in the superfluid state, at slightly lower temperatures and more closely approximating the actual conditions in the EDM experiment.

First evidence of a superfluid bath in the vessel was obtained in early December 2004, and the main volume was eventually filled to the 70% level with no evidence of leakage. This result validates the use of large, commercial wire-seal flanges as a possible technology for holding large volumes of superfluid in the final experiment. However, the custom transfer line failed to replenish superfluid at a rate fast enough to keep the electrodes completely covered for intervals sufficiently long for high voltage tests.

Since the beginning of January 2005, the transfer line has been installed in a small cryostat that can be filled quickly with liquid helium, making for easy testing and design optimization. As soon as this problem is remedied, the transfer line will be reinstalled in

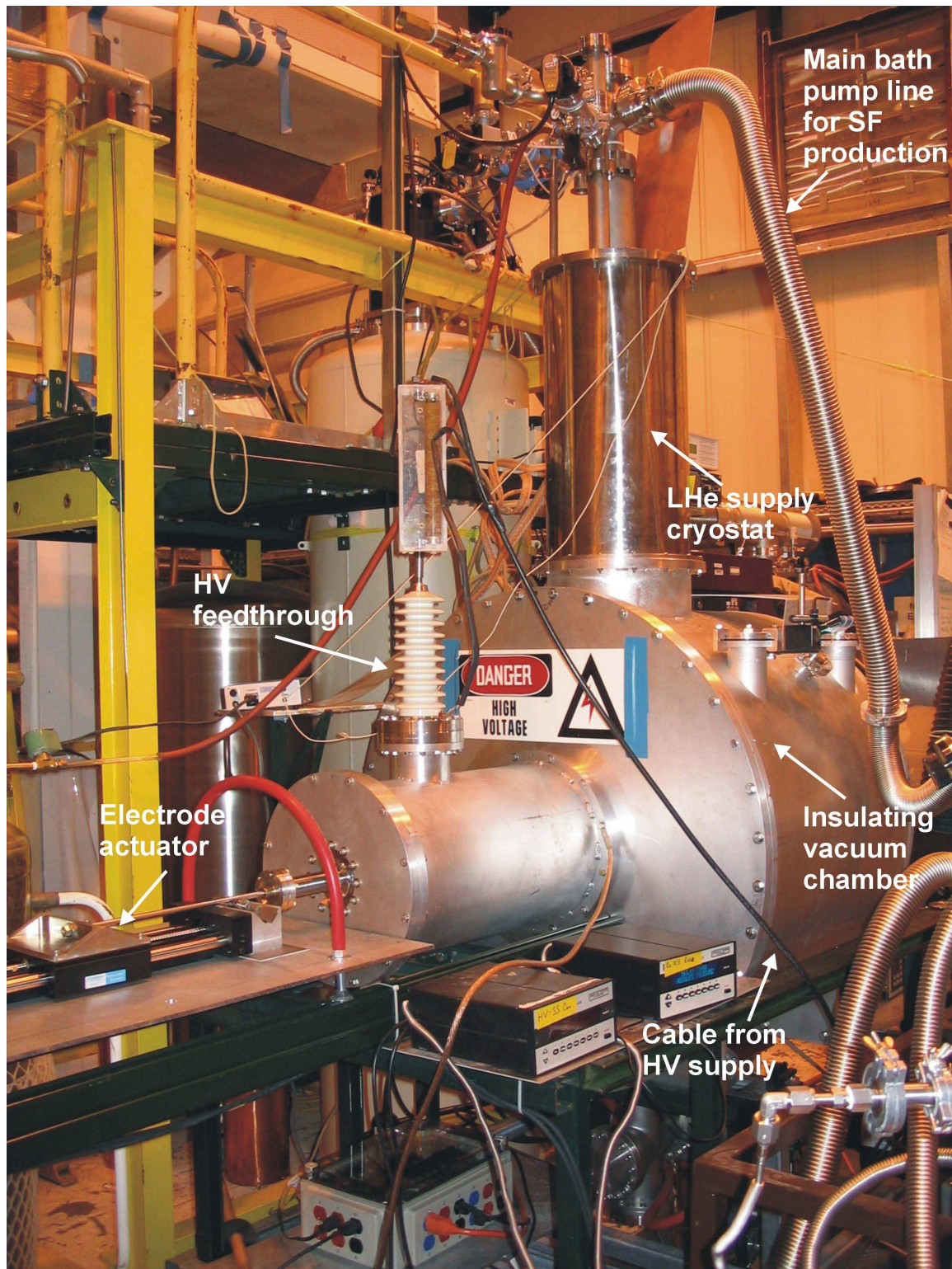


Figure IV.A.1. Complete HV apparatus in EDM test lab at Los Alamos. The variable capacitor and liquid helium vessel are situated within wide part of insulating vacuum chamber. The small vertical cylinder at the top of vacuum chamber is a liquid helium supply reservoir. The white ribbed attachment in front is a commercial feed-through for passing the initial 50 kV potential from a lab power supply into the vacuum chamber. The control rod exiting the chamber on the left connects to an electrode through a bellows just inside the chamber, and on the outside, to an external actuator (shown at far left) for automated control of the electrode position.

the main apparatus, after which results on the basic dielectric properties of large volumes of superfluid can be obtained.

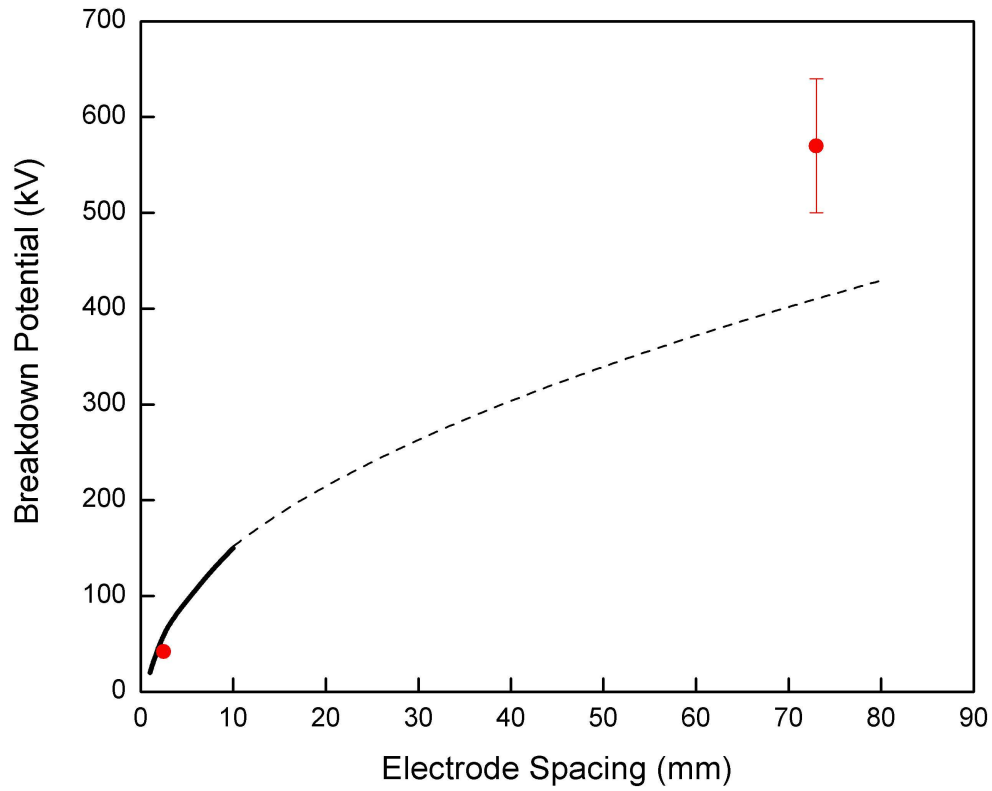


Figure IV.A.2. Experimental results on dielectric strength of liquid helium vs. electrode spacing. Solid line: the trend of data from previous experiments extending out to 10 mm spacing. Dashed line: an extrapolation of old data, in proportion to the square root of the spacing as suggested in EDM pre-proposal, leading to an expected breakdown voltage of 420 kV at 80 mm. Red points at 2.5 mm and 73 mm: the results of this experiment. Point at 73 mm maximum measured potential of 570 kV, approximately 30% higher than expected.

## IV. B. Kerr Effect in Superfluid $^4\text{He}$

The electro-optical Kerr effect describes birefringence induced in an initially isotropic medium by an externally applied electric field,  $E$ . Linearly polarized light propagating in such a medium experiences a different index of refraction when its polarization is parallel to  $E$ , compared to the case when its polarization is perpendicular to  $E$ :

$$\Delta n = n_{\parallel} - n_{\perp} = KE^2,$$

where  $K$  is the Kerr constant of the medium.

The Berkeley group has recently demonstrated the Kerr effect in liquid helium and measured the LHe-Kerr constant,  $K_{\text{LHe}}$ , as a function of temperature in the range 1.5 K to 2.2 K, Fig. IV.B.1.

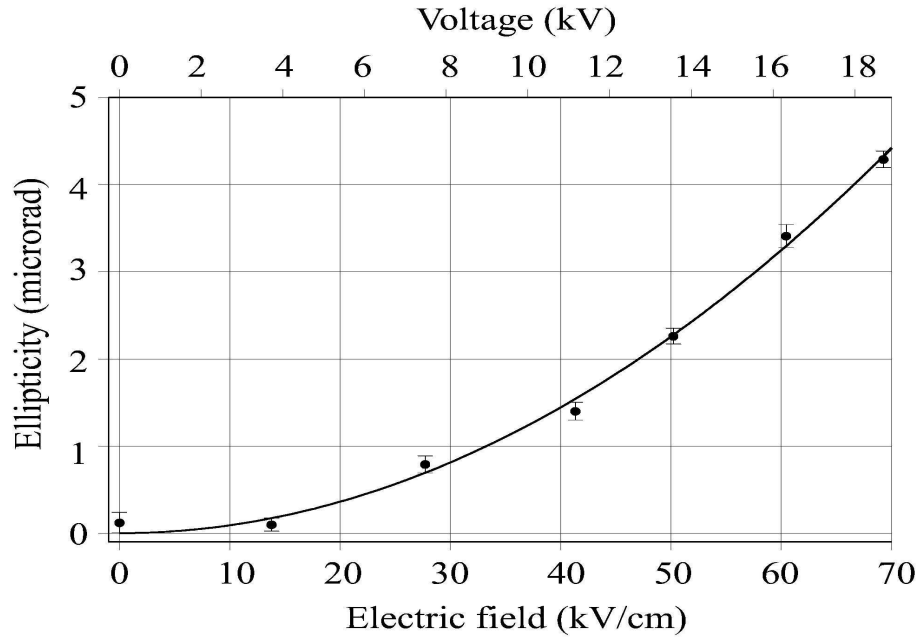


Figure IV.B.1. Kerr Effect observed in superfluid He: Ellipticity in microradians for Electric fields up to 68 KV/cm.

The experimental value for the Kerr constant of superfluid helium at  $T=1.5$  K and saturated vapor pressure is:

$$K_{\text{LHe}} = (1.43 \pm 0.02^{(\text{stat})} \pm 0.04^{(\text{sys})}) \times 10^{-20} \text{ (cm/V)}^2.$$

The measured temperature dependence of the  $K_{\text{LHe}}$  in the range 1.5 K to 2.2 K is shown in the Fig. IV.B.2. A detailed description of the experiment, its results, and some novel conclusions of theoretical significance drawn from these results, can be found in [1].

Having completed the Kerr effect measurements at UC Berkeley, efforts are under way to set up a laser polarimeter for using the Kerr effect to measure electric fields in the LANL High Voltage Variable Capacitor apparatus, Fig. IV.A.1. This will allow a direct application of the Kerr effect to measuring the electric field in nearly the same configuration as in the neutron EDM experiment. We expect that the measurement time will be reduced in inverse proportion to the path length of the laser beam.

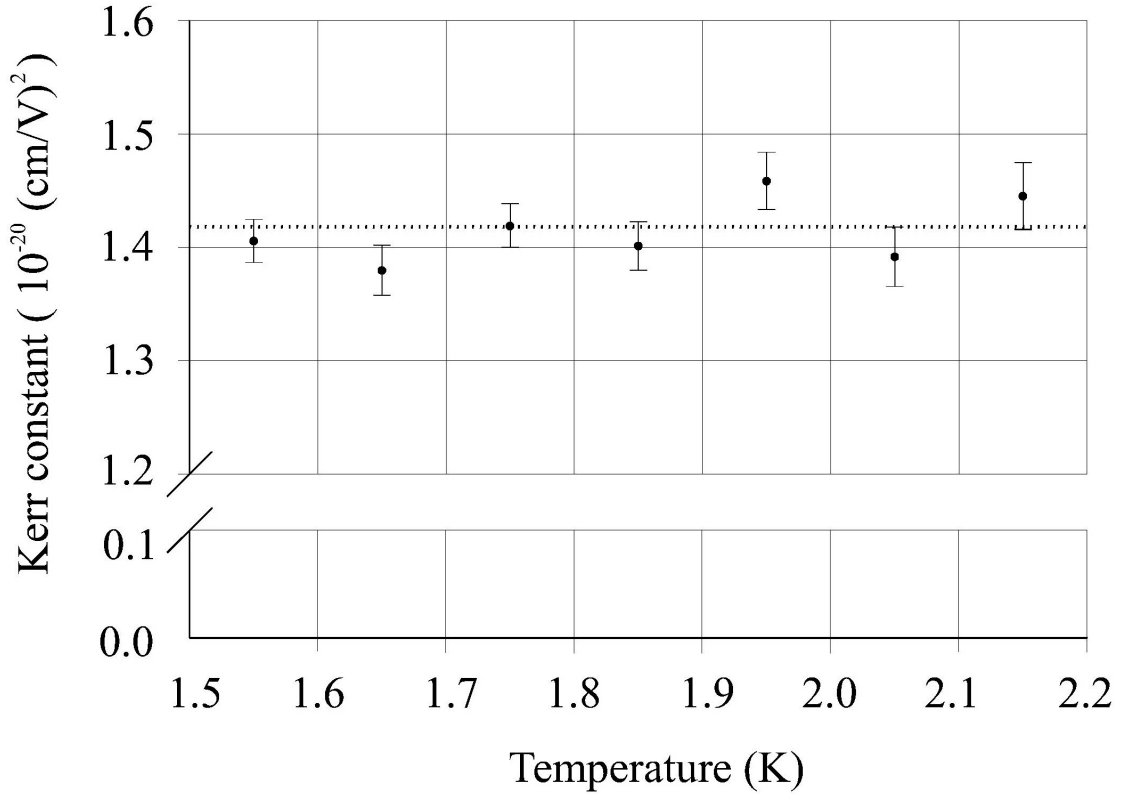


Figure IV.B.2. Temperature dependence of the Kerr Constant in superfluid liquid helium.

- [1] A. O. Sushkov, E. Williams, V. V. Yashchuk, D. Budker, and S. K. Lamoreaux, Kerr effect in liquid helium at temperatures below the superfluid transition, Phys. Rev. Lett. **93**, 153003 (2004).

## IV.C. Magnetic Fields and Magnetic Shielding

Detailed studies have been underway at Los Alamos and Caltech to investigate magnetic field uniformity and magnetic shielding in the lower cryostat of the EDM experimental apparatus. The holding (static) field for the polarized neutrons and  $^3\text{He}$  is required to be a 1-10 mG field with a uniformity of  $10^{-3}$  over the volume of the measurement cell. Stray fields must be expelled to ensure that this spacial uniformity is achieved and is stable in time. In the pre-proposal we discussed the use of a superconducting shield around the holding-field coils (assumed to be of the  $\cos-\theta$  type). However this configuration introduces several design challenges to the experiment. They arise from the large volume required for the shield needed to maintain the field uniformity, as driven by the magnetic boundary conditions at the surface of the superconductor. In addition, trapped fields in the superconductor can lead to systematic problems.

We have explored installing a low temperature ferromagnetic shield inside the superconducting shield, in order to alleviate these problems. All previous EDM experiments have relied on ferromagnetic shields, but due to the presence of the liquid He we are required to operate the innermost shield at low temperature. It is well known that the conventional magnetic shielding material – mu-metal – loses much of its shielding effectiveness at such low temperatures. We have investigated two promising materials, Metglas and Cryoperm, which both appear to maintain a very high permeability even in these temperatures ranges. Their thermo properties appear to resolve the problematic issues associated with the holding coil inside of a superconducting shield.

We have also explored different holding-coil configurations in order to optimize the EDM design. Using boundary condition calculations and prototype coil measurements inside of ferromagnetic shields, we have been able to show that modest length coils can be used with open end-caps for the holding coil. Recall that a conventional  $\cos-\theta$  magnet has a fixed pitch for the wire spacing when measured along the axis of the magnetic field. For a coil wrapped around a right cylinder this would result in the end-caps covered with the evenly spaced wires. However we have demonstrated, both experimentally and theoretically, that the end-cap wires can be wound in a circle with fixed radius equal to the cylinder's radius. This allows for easy access of services through the magnet and into the measurement volume.

A critical issue in the design of the experiment is the measurement of the precession of the neutron spin. The dressed-spin technique, described in section II.B, will be used to provide an alternate technique to the SQUID detector method of measuring the spin precession. A RF field coil is required in addition to the coil for generating the static B field. However utilization of a single magnet would produce an unacceptable heat load due to Eddy currents in the shield. Thus, we are allowing extra space for a nested pair of bucking RF (dressed spin) coils to perform this operation, whose fields nearly cancel out in the larger radius region near the ferromagnetic shield (the 0.3 K region).

The constant field  $\cos-\theta$  coil lies outside the dressed-spin coils in order to accommodate the ferromagnetic shield, which provides the correct boundary conditions for the static

field coil, Fig. IV.C.1. The superconducting shield has been moved outward. Addition of these extra elements has substantially increased the size of the lower cryostat to a length of 8.4 m and a diameter of 3.2 m.

We are presently preparing to construct 1/8-scale prototypes of the static field magnet, the ferromagnetic shield, and the dressed spin coils, to assess the performance of the apparatus. These tests include magnetic field mapping and cryogenic performance.

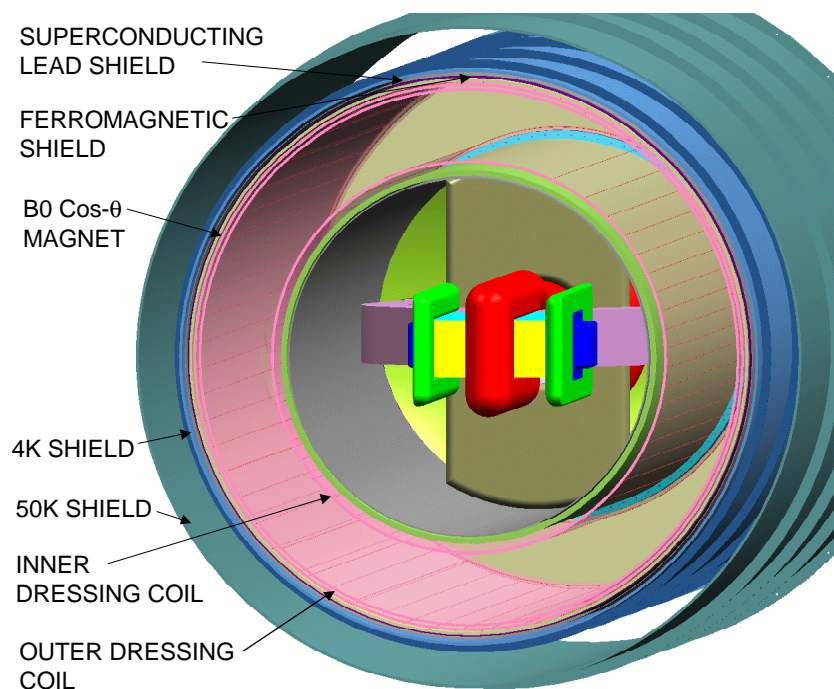


Figure IV.C.1. Nested set of (two) dress spin coils, static field coil, ferromagnetic shield, and superconducting shield in the lower cryostat. The three electrodes surrounding the two experimental cells are shown at the center.

#### IV. D. Tests and Performance of the $^3\text{He}$ Atomic Beam Polarizer

Final testing and qualification of the  $^3\text{He}$  atomic beam polarizer (ABP), Fig. IV.D.1, were completed in November 2004. The design specifications were fully met.

Two separate methods were used to determine the  $^3\text{He}$  atomic flux, and both indicate that  $4 \times 10^{14}$  atoms /sec are delivered at the output of the polarizer. This measured flux was at the expected value and met the requirements of the EDM experiment. The time to collect the necessary number of atoms for a single filling of the experimental cells (8 liters,  $^3\text{He}$  concentration  $10^{+13}$  /cc) is 75 seconds, much shorter than the anticipated measurement cycle of 2000 s.

The degree of polarization was determined through a combination of a radiofrequency spin-flip technique and a subsequent transmission measurement through a quadrupole analyzer identical to the polarizer. This method also provides a measure of the Fourier transform of the velocity spectrum. This spectrum was inverted to give the velocity spectrum (solid curve) in Fig. IV.D.2. The measured spectrum is consistent with a 1 K Maxwell-Boltzmann distribution (dotted curve). Note that the flux below  $\sim 1 \times 10^4$  cm/sec is distorted due to velocity-dependent defocusing effects in the quadrupole polarizer and analyzer.

The degree of polarization is  $99.6 \pm 0.2\%$ , after subtraction of a very small background that was determined by independent means. This background will be completely eliminated by addition of a second differential pumping stage to the apparatus.

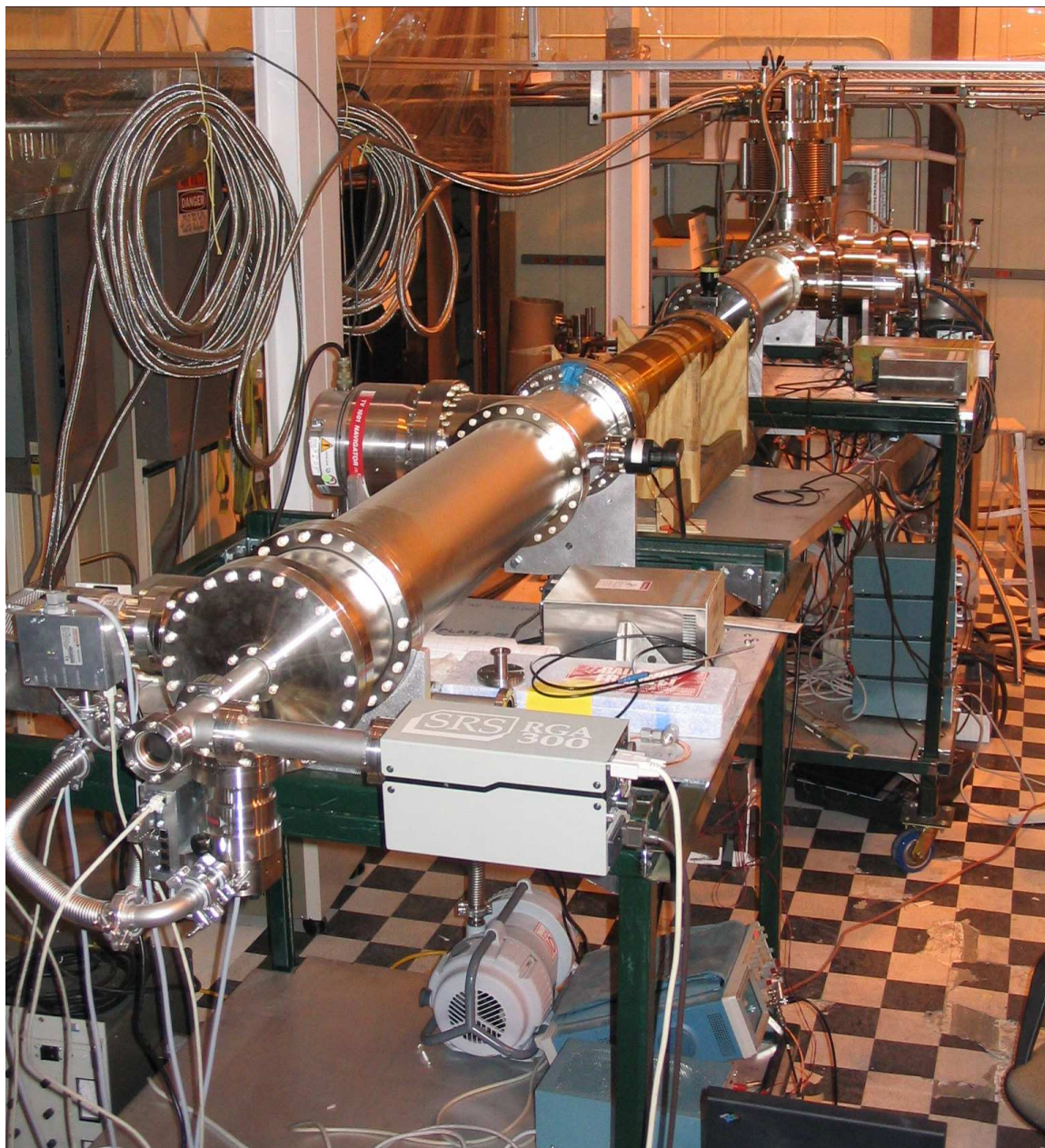


Figure IV. D.1. The  $^3\text{He}$  Atomic Beam Polarizer (ABP) apparatus

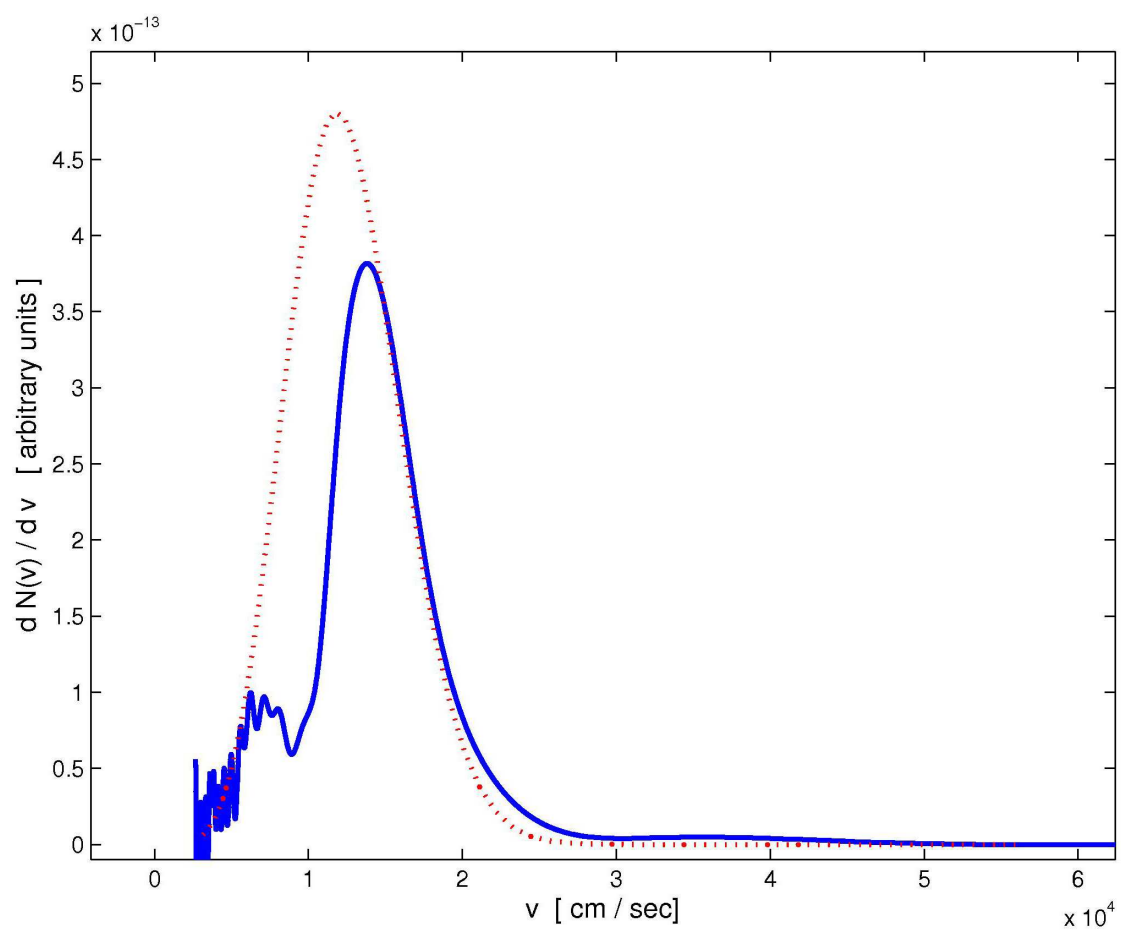


Figure IV.D.2. Measured velocity distribution (solid curve) compared to a 1 K Maxwell-Boltzmann distribution (dotted curve).

## IV.E. $^3\text{He}$ Cell Studies

The design goal for the  $^3\text{He}$  relaxation time,  $\tau_3$ , in the neutron cells of the EDM experiment, is 30,000 s. For reference a degraded  $\tau_3$  of 3,000 s will contribute a factor of 1.9 to the loss of EDM sensitivity.

A  $^3\text{He}$  polarizer based on the Spin Exchange Optical Pumping (SEOP) technique has been built at Duke, Fig. IV.E.1, together with a double glass (GE180) valved system and a dual NMR system to provide a baseline measurement of  $\tau_3$  for the EDM experiment. An SEOP produces many more polarized atoms than an ABP but with reduced polarization, and provides an easily detected signal. The double-cell system allows the test cell to be coated with deuterium,  $^4\text{He}$ , or d-TPB. The latter is achieved with acrylic sticks coated with d-TPB wavelength shifting material, placed inside the cell and permit study of the effect of the d-TPB material on  $\tau_3$  down to a temperature of 2.4 K.

With a 21 G holding field, relaxation times of 13,900 s at 4.2 K and 30,000 s at 2.5 K have been obtained using a sealed cell filled with 100 torr of  $^3\text{He}$ , 50 torr of  $\text{N}_2$  and 525 torr of  $^4\text{He}$  at room temperature. The  $\tau_3$  was 36,000 s at 300 K under the same holding field. The longest relaxation time, 7 to 8 hours at room temperature with a 7 G holding field, has been achieved for a double-cell system filled with 2200 torr  $^3\text{He}$  and 100 torr  $\text{N}_2$ . A complete test under a holding field of 7 G to determine the relaxation time due to the d-TPB coated surfaces, was carried out and achieved a relaxation time of 3200 s at 300 K. The extracted  $^3\text{He}$  relaxation time due to d-TPB coated acrylic surfaces (a total surface area of 25.9 cm<sup>2</sup>, ~ 31% of the GE180 test cell surface area.) is  $3800 \pm 1300$  s at 2.4 K.

Longer relaxation times are expected to be achieved with better baseline relaxation time. Several tasks remain to be done:

- (1) Reduce measurement errors in deducing the  $^3\text{He}$  relaxation time on d-TPB coated acrylic surfaces,
- (2) Measure  $^3\text{He}$ -relaxation time in an acrylic test cell coated with d-TPB at temperatures below the Lambda point.

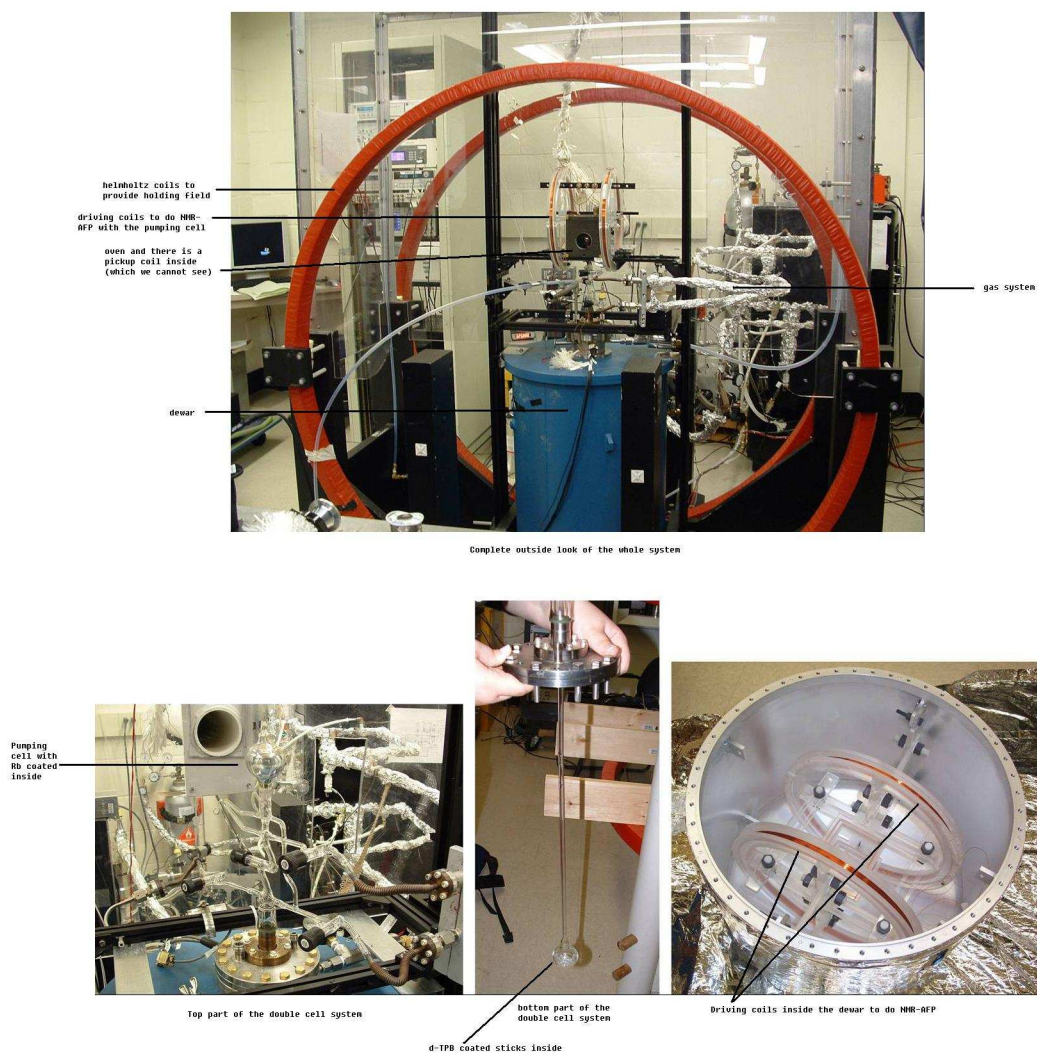


Figure IV.E.1 Test apparatus at Duke University for  $^3\text{He}$  cell relaxation time studies.

## IV. F. Reservoir for Purification of Superfluid $^4\text{He}$

A critical experimental issue for the EDM apparatus is how, after a measurement cycle, to purify the reservoir of  $^4\text{He}$  of depolarized  $^3\text{He}$  in the upper cryostat. We had considered using the McClintock heat-flush technique, but the impure superfluid  $^4\text{He}$  would have to be heated to a temperature of about 1 K for this technique to be effective. The heat load associated with this heating and subsequent re-cooling to 0.3 K would be excessive, so we revisited an idea that had been considered previously.

The new strategy, Fig. IV.F.1, is to simply drain the contaminated superfluid,  $^4\text{He}$ , into a holding chamber with a vacuum space above the liquid. We then simply let the  $^3\text{He}$  atoms evaporate into this space and then pump the atoms away, with a cryogenic charcoal pump above the liquid.

We have addressed several issues regarding the practicality of this technique. The minimum temperature where the evaporation purification process could be performed in a time scale compatible with the experiment cycle (2000 s) was determined to be 0.3 K. This temperature was determined by considering the fraction of  $^3\text{He}$  atoms in the liquid (assuming a Maxwell-Boltzmann distribution) with sufficiently high velocity normal to the surface to overcome the binding energy in the liquid (2.8 K), and accounting for the surface reflection coefficient. On the other hand, the maximum temperature was determined by the onset of diffusive motion (due to phonon scattering) instead of ballistic motion of the  $^3\text{He}$  atoms. For a detailed discussion of the temperature dependence of  $^3\text{He}$  mobility in superfluid  $^4\text{He}$  see [1]. This temperature was determined to be 0.6 K, so there is a 0.3 K wide temperature window where the evaporative technique should work.

We also considered the binding of  $^3\text{He}$  atoms into surface states in the liquid. For the temperatures listed above, the fraction of  $^3\text{He}$  atoms bound in these states is very small. However, at temperatures below 0.1 K, a majority of the atoms are trapped in these states, and might serve as the basis of an alternative purification technique.

The final issue to be considered is the design of the charcoal cryopump needed for the evaporative purification. We have modeled a promising engineering design that can be heated in situ (to 4-5 K) to remove superfluid  $^4\text{He}$  films and will be isolated from the bath by use of cesium films or film burners on the support structure.

We are planning to experimentally test these techniques over the next year or so.

[1] S.K. Lamoreaux et al, "Measurement of the  $^3\text{He}$  mass coefficient in superfluid  $^4\text{He}$  over the 0.45-0.95 K temperature range," Europhysics Letters 58, 718 (2002).

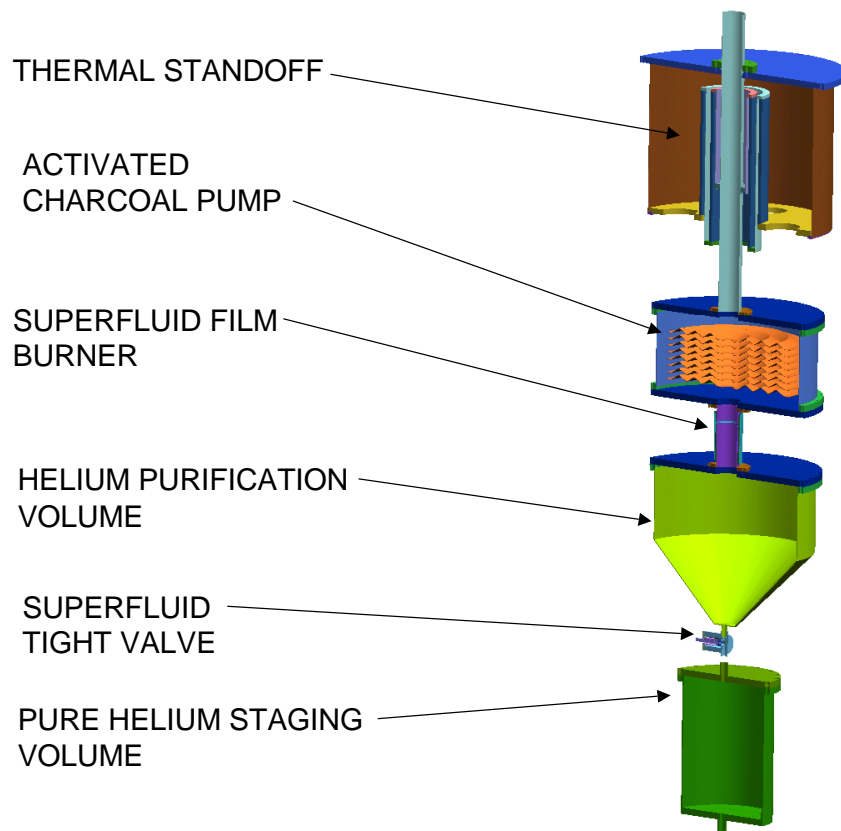


Figure IV.F.1. Layout of the  $^4\text{He}$  purification volume and the staging volume in the upper cryostat. This is to the right of the sample preparation volume and its  $\cos\theta$  magnetic coil in Fig. II.A.2.

## IV.G. Background Issues

The maximum sensitivity to an EDM signal is obtained by minimizing the ratio of background events to neutron capture events on  $^3\text{He}$ . Background events arise from a number of sources: decay of bottled UCN, neutron-induced activation of surrounding materials, cosmic rays, and external radiation to name a few. Of these, cosmic rays can be vetoed using external scintillators. The remaining sources must either be minimized by judicious choice of materials combined with shielding or using discrimination techniques. We are in the process of investigating both these techniques though measurements performed at the National Institute of Standards and Technology (NIST) reactor facility and at the Hahn-Meitner Institut (HMI) cold neutron beam facility.

The test run at NIST showed that neutron-induced activation due to the beam passing through and being stopped by the acrylic walls of the cell does not appear to create significant backgrounds at the present level of sensitivity. However care must be taken to minimize any neutron activating-materials in the vicinity of the beam and detection cells.

With regard to the scintillation light spectrum in liquid Helium, the possibility of tagging direct neutron capture on  $^3\text{He}$  in LHe at  $T = 1.8\text{K}$  has been reported [1] using an after-pulse measurement technique. The method of after-pulse discrimination is a pulse shape technique implemented by plotting the number of single photoelectrons detected in the 7  $\mu\text{s}$  bin following the main scintillation pulse versus the total area of the scintillation light signal. If the scintillation light produced by other mechanisms, for example neutron beta decay or gamma ray induced events can be discriminated against, the tagged scintillation signal for the desired neutron capture, has the possibility of being nearly background free, increasing the sensitivity of the measurement. The events due to  $^3\text{He}$  neutron capture produce more highly ionizing particles as compared to the low ionizing beta particles from neutron decay. The highly ionizing particles excite different dimers in the  $^4\text{He}$  than the betas, leading to a light component with a longer de-excitation time and different number of after-pulses.

At HMI the specific test was to explore the feasibility of using correlations between the size of the scintillation pulse and the number of after-pulses for a given event due to  $^3\text{He}$  neutron capture at temperatures relevant to an EDM measurement. Recent studies at NIST for alpha-particles showed a temperature dependence in the after-pulse rate; the number of after-pulses decreases as the temperature is lowered below 1.9 K [2].

The HMI measurements were performed in a  $^3\text{He}/^4\text{He}$  liquid sample around the proposed EDM operating temperature of approximately 300 mK. The  $^3\text{He}/^4\text{He}$  fractional concentration was chosen such as to provide total detector count rates from 0.4 kHz (similar to the expected EDM count rate) to 10 kHz. The light collection system resembled a small-scale version of the present EDM design: an acrylic cell about 5 diameters long with a light guide attached to each end of the cell. The beam passed through the cell perpendicular to the long axis in the central region, at a right angle to the light collection system. In contrast to both the previous NIST test run and to the current EDM design, we

have a fixed geometrical detection efficiency that allows us to study a neutron capture peak with better resolution.

Detailed analysis of the data is in progress. Nevertheless, we can draw several important conclusions:

i) Having two separate light guides looking at the same cell allowed us to detect a neutron peak (700 Hz) with a neutron beam of intensity of  $1 \times 10^4/\text{s}$  entering the cell. The neutron beam creates a strong background from prompt gammas and high energy betas from Al-28 beta-decay. The background rate under the neutron capture peak was 1200 Hz without the coincidence requirement, and decreasing to 300 Hz with the coincidence requirement between the two PMTs. Thus use of the coincidence technique allowed us to suppress backgrounds by a factor of four. We find that the use of the coincidence technique is critical for the EDM design.

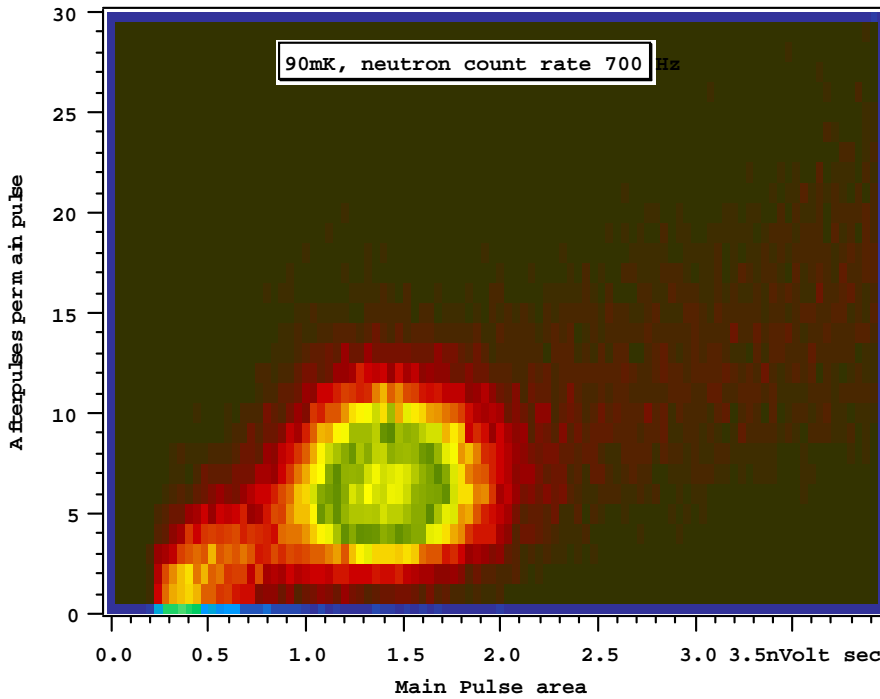


Figure IV.G.1. The measured separation between n-<sup>3</sup>He capture events and low energy beta's and gamma's at 90 mK: number of after-pulses as a function of pulse area.

ii) additional improvement of the background separation is obtained using a two-parameter analysis. In Fig IV.G.1, events are displayed on a 2D contour plot, graphing the number of after-pulses as a function of pulse area at lowest temperature  $T=90$  mK. A deep valley appears on the 2D plot between the higher-energy peak of the neutron-<sup>3</sup>He capture events and the low energy peak from the gamma and beta background events.

This valley is absent in the single-parameter pulse area spectrum.

iii) The maximum area of a neutron capture event is found to be approximately 20 times that of a single photo-electron event (s.p.e.) providing an excellent separation from low energy gammas and betas in our geometry. These values look very promising for the future EDM cell, where the geometry of the cell will spread the neutron peak to lower amplitudes. With an efficiency of 50% in our present setup, the neutron EDM cell should have a neutron peak maximum 10 times that of a s.p.e. At such low amplitudes only the two-parameter contour technique described above will allow us to achieve a clean separation of  $n$ - $^3\text{He}$  capture events from the gamma ray events.

[1] K. Habicht, PhD Thesis, Technische Universität Berlin (1998).

[2] D. N. McKinsey, C. R. Brome, S. N. Dzhosyuk, R. Golub, K. Habicht, P. R. Huffman, E. Korobkina, S. K. Lamoreaux, C. E. H. Mattoni, A. K. Thompson, and J. M. Doyle, Time dependence of liquid helium fluorescence, *Physical Review A*, **67**, 062716 (2003)

## IV. H. $^3\text{He}$ Polarization Losses in the $^3\text{He}/^4\text{He}$ Sample Preparation Volume

Analysis of  $^3\text{He}$   $T_1$  Depolarization in the Collection Volume and Transfer Tube and  
Experimental Volume:  
Magnetic Field Homogeneity Requirements

With many features of the conceptual engineering design worked out, it is now possible to address the issue of losses of  $^3\text{He}$  polarization in the  $^3\text{He}/^4\text{He}$  sample preparation volume, (upper cryostat,) and the target volume (lower cryostat).

This problem is different from the usual one encountered in low field magnetic resonance, because we are working with very small fields and we are operating near the limit between ballistic and diffusive propagation of  $^3\text{He}$  in the superfluid helium bath. We take the diffusion coefficient for  $^3\text{He}$  motion against phonons ( $^3\text{He}$  -  $^3\text{He}$  collisions do not contribute significantly at the concentrations we are considering),  $D = 1.8 \times 10^{-7} \text{ cm}^2/\text{s}$  from our previous measurement [1]. For  $T = 0.35 \text{ K}$ ,  $D = 3 \times 10^{-7} \text{ cm}^2/\text{s}$ . Using

$$D = \lambda v / 3$$

and  $v = 3600 \text{ cm/s}$  (effective  $^3\text{He}$  mass in superfluid  $^4\text{He}$  is  $2.2m_3$ ), implies a mean free path between collisions,  $\lambda = 2.3 \text{ cm}$ . For the sample preparation volume of Fig II.A.2, we imagine a 20-liter capacity filled with superfluid helium that will collect polarized  $^3\text{He}$  atoms from the ABP. Assume a cylinder, 30 cm diameter, and 30 cm high that contains the superfluid helium plus a small component of  $^3\text{He}$ . The ballistic mean free path is determined by the ratio of the volume to surface area,

$$L = 4V/S = 27\text{cm}.$$

From the known ABP flux, section IV.D., the time required to collect the polarized  $^3\text{He}$  is about 200 sec.; we assume the collection time can be limited to this period (see [3] below). This volume then feeds the UCN measurement cells through a tube of 1 cm diameter and 100 cm long. The transfer should take less than 20 sec. so any particular  $^3\text{He}$  atom will be in the transfer region for less than three seconds. After the experimental cells are filled with polarized  $^3\text{He}$ , the spin flip occurs within 10 sec. However, the total storage time in the experimental cells is about 1000 seconds when the time to collect the neutrons is included.

We therefore must analyze the field homogeneity requirements in three different regions: the  $^3\text{He}$  sample preparation volume (Fig II.A.2 just below the region shown in Fig. IV.F.1), the transfer tube, and the experimental cells shown in Fig. IV.C.1.

### Sample Preparation Volume

From the above considerations, the diffusive limit is applicable to the main collection volume. The time to travel one cell mean free path is

$$L = [2D \tau_d]$$

which implies  $\tau_d = 0.1$  sec. We consider holding fields of at least  $B_0 = 10$  mG, so  $\omega_0 \tau_d = 9 \gg 1$ . In this limit, Eq. (58) of [2] is applicable,

$$1/T_1 = (D/B_0^2) (|\nabla B_x|^2 + |\nabla B_y|^2) \quad (1)$$

with  $B_0$  assumed to lie along the z axis and  $B_{x,y}$  are the transverse (gradient) fields. This assumes that the gradients and  $B_0$  are constant through the volume.

To have at most a 1% polarization loss in the sample preparation volume, we need a lifetime of 20,000 sec. Defining  $[(dB_x/dx)^2 + (dB_y/dy)^2] = dB_r/dr = \alpha$  for a constant  $dB_z/dz$ , and  $\Delta B_r = \alpha R$ , Eq. (1) implies a maximum gradient of:

$$5 \times 10^{-5} < (3 \times 10^{-3} \text{ cm}^2/\text{s}) (\alpha/B_0)^2 \rightarrow \alpha/B_0 < 1.3 \times 10^{-4} / \text{cm}$$

This requirement is further relaxed if the time between velocity changing collisions,  $\tau_c$ , is such that  $\omega \tau_c \gg 1$  and the relaxation rate will be further suppressed as  $1/(1+(\omega \tau_c)^2)$ . Taking  $\lambda = v \tau_c$ , we see, under the conditions assumed, that  $\tau_c = 6 \times 10^{-4}$  s, which implies a field of 83 mG before this suppression factor kicks in. Thus the requirement is that the field is homogeneous to 0.2% in the collection cell, assuming a holding field of less than 100 mG.

### Transfer Tube

We assume  $^3\text{He}$  will be kept out of the transfer tube until the transfer actually takes place. If the transfer tube is 1 cm diameter, then the mean free path is about 1 cm, so  $\tau_c = 3 \times 10^{-4}$  s. Again, due to the short time between wall collisions, we expect to always be in the low field regime. The  $T_1$  lifetime should be more than 200 sec (1% polarization loss in less than the 2 seconds that a  $^3\text{He}$  atom spends in the transfer tube, as described in

the introduction). In this region, because the phonon collision mean free path is longer than the ballistic mean free path, Eq. (66) of [4] is applicable; in the small  $\tau_c$  limit

$$T_1^{-1} = \gamma^2 R^2 \alpha^2 \tau_c / 2$$

where  $\gamma$  is the gyromagnetic ratio, Hz/mG, and  $R$  is the tube radius. The limit for  $\alpha$  is therefore

$$\alpha < 1.8 \text{ mG / cm}$$

which should be easy to achieve.

On the other hand, if we want to tailor a strong holding field on the sample preparation volume to a small field at the experimental cell region inside the magnetic shields, there is a constraint on the maximum rate of change of  $B_0$ . If we imagine a long straight tube, and if we vary  $B_0$  along the length, say by winding a solenoid with varying pitch, the radial gradient is given simply by  $dB_z/dz = \alpha$  as described above. It therefore seems possible to have a relatively high field at the sample preparation region that is tailored to the low field at the experimental cells.

### Experimental Cell:

The  $T_1$  gradient requirements are similar to what is required for  $T_2$  in the experimental cell. These are worked out in the Physics Report article [5].

Footnotes and References:

- [1] S.K. Lamoreaux et al., “Measurements of the  $^3\text{He}$  mass coefficient in superfluid  $^4\text{He}$  over the 0.45 – 0.95 K temperature range,” Europhysics Letters 58, 718 (2002).
- [2] G.D. Cates, S.R. Schaefer, and W. Happer, Phys. Rev. A 37, 2877 (1988).
- [3] The limits for the collection volume size have not been addressed. We could imagine operating the experiment as follows: fill the experimental measurement volume nearly full (fraction  $\beta$ ) of ultra pure superfluid  $^4\text{He}$ , and have the  $^3\text{He}$  collection volume equal to the unfilled fraction  $(1 - \beta)$ . The limit for the collection cell volume is determined by: i) maximum allowable concentration before phase separations sets in (concentration  $x = 0.4$ ); ii)  $^3\text{He}$ - $^3\text{He}$  diffusion, which becomes equal to the phonon diffusion at 0.4 K when  $x = 10^{-7}$ . We require  $x = 10^{-10}$  in the experiment cells so in fact the collection volume could be more than 100 times smaller than the experimental volume.
- [4] D. Kleppner, H.M. Goldenberg, and N.F. Ramsey, Phys. Rev. 126, 603 (1962).
- [5] R. Golub and S. Lamoreaux, Phy. Rep. 237, 1 (1994).

## V. Additional Investigations in Progress

This report has focused on a series of technical issues related to the design and construction of the neutron EDM measurement apparatus. For the investigations discussed, most of the crucial results have been obtained. The baseline design has been evaluated in the context of the results from these critical technical studies. The resulting design changes have now been incorporated into the conceptual engineering design of the experimental apparatus.

In this section we list a number of projects that are currently under study and that will provide further verification and improvement of the technical approach adopted for this measurement of the neutron electric dipole moment.

1. Neutron storage time tests with EDM cell wall materials at the LANL UCN source.
2. Simulation and design of the SNS neutron beam splitter/spin filter
3. Dynamic tests of the  $^3\text{He}$  injection and sample preparation system using the polarized  $^3\text{He}$  Atomic Beam Source now constructed.
4. Test of the  $^4\text{He}$  purification technique using the direct pumping method.
5. Investigation of the impact of super-mirror neutron guides on magnetic field uniformity.
6. A measurement of  $^3\text{He}$  polarization relaxation times below 1 K.
7. Development of a superfluid tight valve capable of  $10^5$  automated cycles.

The collaboration has submitted an R&D proposal to DOE to complete the above program and to undertake some other investigation for future improvements.

## VI. Conclusions

Over the past three years the EDM collaboration has conducted a series of conceptual studies, engineering design projects, and direct tests in the laboratory that have led to a well thought out and verified base line design for the experiment. The technical risks factors identified previously have now been addressed and have acceptable solutions. The residual risk is now within acceptable bounds, and the continuing research will further reduce it. The sense of the collaboration is that there are no technical “show-stoppers” in the concept of the experiment.

This project is in the process of evaluating improved technologies and solving challenging engineering problems. These tasks are moving ahead as permitted by R&D funds. The base design, presented in the pre-proposal and in this update report, is judged to represent an excellent framework for development of an overall cost and schedule for this project at this pre-conceptual phase.